Journal of Molecular Structure 1261 (2022) 132939

Contents lists available at ScienceDirect

Journal of Molecular Structure

journal homepage: www.elsevier.com/locate/molstr

Determination of the effect of *L. plantarum* AB6-25, *L. plantarum* MK55 and *S. boulardii* T8-3C microorganisms on colon, cervix, and breast cancer cell lines: Molecular docking, and molecular dynamics study

Seda Yalçınkaya[a], Serap Yalçın Azarkan[b,*], Aynur Gül Karahan Çakmakçı[a]

[a] Department of Food Engineering, Faculty of Engineering, Süleyman Demirel University, Isparta 32260, Turkey
[b] Department of Molecular Biology and Genetics, Faculty of Art and Sciences, Kırşehir Ahi Evran University, Kırsehir 40100, Turkey

ARTICLE INFO

Article history:
Received 28 January 2022
Revised 24 March 2022
Accepted 25 March 2022
Available online 28 March 2022

Keywords:
Cancer
Apoptosis
Probiotics
Molecular docking
Molecular dynamic

ABSTRACT

Cancer constitutes an important part of the diseases that are caused all over the world. Due to the side effects of commonly used treatment options such as chemotherapy and radiotherapy, there has been a tendency to seek natural anticancer compounds. In this study, the cytotoxic effects of *L. plantarum* AB6-25, *L. plantarum* MK55, and *S. boulardii* T8-3C probiotic strains on HCT-116, HeLa, and MDA-MB-231 cell lines were determined. The effect of the microorganisms' cell contents was also evaluated in 3D cancer cell lines. To evaluate the effect of microorganisms on metastasis, we applied to wound healing and invasion assays. At the same time, the cytotoxic effect of microorganisms on cancer cell lines was determined at the gene level using Real-Time qPCR. In addition, the effect of microorganisms on the expression of CASP3 protein in HeLa cells was also evaluated. At the last stage of the study, molecular docking and molecular dynamics simulation studies were carried out with the microorganism metabolites detected by QTOF-LC/MS. The results of the study showed that the most effective strain on HeLa and MDA-MB-231 cells was *L. plantarum* AB6-25 with a 91% and 80% inhibition rate, respectively, while *L. plantarum* MK55 had the highest cytotoxic effect on HCT-116 cells with a 69% inhibition rate. On the other hand, *S. boulardii* T8-3C had a weaker anticarcinogenic effect on cancer cell lines compared to the other two bacteria. According to the migration and invasion assays results, HCT-116 and MDA-MB-231 cells were the most effective bacteria in preventing *L. plantarum* MK55, and *S. boulardii* T8-3C metastasis in HeLa cells. As a result of gene expression analysis, microorganisms showed the greatest effect on apoptotic genes in HeLa cells. In HCT-116 and MDA-MB-231 cells, the expression level of apoptotic genes changed less. In the western blot analysis, *L. plantarum* AB6-25, *L. plantarum* MK55, and *S. boulardii* T8-3C cell contents expressed CASP3 at a higher level in the 2D HeLa cells compared to the 3D cells. The *BAX* protein and istamycin C1 ligand, which resulted in the binding energy of -8.23 kcal/mol, were determined as the molecules with the best anti-cancer effect. The results of *in vitro* studies have been supported by genetic expression analysis and molecular docking studies, and have shown the potential of microorganisms' cell contents to be an anticancer agent.

1. Introduction

The most commonly used chemotherapy and radiotherapy methods in cancer treatment usually cause serious side effects in patients [1]. For this reason, investigations have been carried out on natural substances and organisms with anticancer effects in recent years. In this context, it is seen that studies on the effects of probiotics, which have many benefits on health and various types of cancer, have been published. Anticancer action mechanisms of probiotics can be grouped under 4 headings: effect on the immune system, removal of carcinogens, enzyme inhibition, and effect on gene expression (antigenotoxicity).

It has been suggested that approximately 20% of colon cancers are caused by microbial infection. It has been stated that pathogens affect the formation of cancer by causing the deformation of epithelial cells and instability in the resident microbiome. In addition, they can cause colon cancer by inducing epithelial DNA damage and tumor formation [2]. It is stated that the resident microbiota and the metabolites they produce have a protective effect against colon cancer [3]. It is known that the metabolites produced

* Corresponding author.
E-mail address: syalcin@ahievran.edu.tr (S. Yalçın Azarkan).

https://doi.org/10.1016/j.molstruc.2022.132939
0022-2860/

Table 1
Primers used in real-time qPCR analysis.

Primer	Primer Sequence	Primer	Primer Sequence
Akt1-F	AGCGACGTGGCTATTGTGAAG	GAPDH-F	GGAGCGAGATCCCTCCAAAAT
Akt1-R	GCCATCATTCTTGAGGAGGAAGT	GAPDH-R	GGCTGTTGTCATACTTCTCATGG
P53-F	GAGGTTGGCTCTGACTGTACC	*BAX*-F	CCCGAGAGGTCTTTTTCCGAG
P53-R	TCCGTCCCAGTAGATTACCAC	*BAX*-R	CCAGCCCATGATGGTTCTGAT
FADD-F	GTGGCTGACCTGGTACAAGAG	BCL2-F	GGTGGGGTCATGTGTGTGG
FADD-R	GGTAGATGCGTCTGAGTTCCAT	BCL2-R	CGGTTCAGGTACTCAGTCATCC
BAD-F	CCCAGAGTTTGAGCCGAGTG	CAS6-F	ATGGCGAAGGCAATCACATTT
BAD-R	CCCATCCCTTCGTCGTCCT	CAS6-R	GTGCTGGTTTCCCCGACAT
BAK1-F	CATCAACCGACGCTATGACTC	CAS8-F	TTTCTGCCTACAGGGTCATGC
BAK1-R	GTCAGGCCATGCTGGTAGAC	CAS8-R	GCTGCTTCTCTCTTTGCTGAA
BRAF-F	TGGGGAACGGAACTGATTTTTC	CASP3-F	CATGGAAGCGAATCAATGGACT
BRAF-R	TTTTGTGGTGACTTGGGGTTG	CASP3-R	CTGTACCAGACCGAGATGTCA
PUMA-F	GACCTCAACGCACAGTACGAG	CASP4-F	CAAGAGAAGCAACGTATGGCA
PUMA-R	AGGAGTCCCATGATGAGATTGT	CASP4-R	AGGCAGATGGTCAAACTCTGTA
NOXA-F	ACCAAGCCGGATTTGCGATT	CASP9-F	CTTCGTTTCTGCGAACTAACAGG
NOXA-R	ACTTGCACTTGTTCCTCGTGG	CASP9-R	GCACCACTGGGGTAAGGTTT
BID-F	ATGGACCGTAGCATCCCTCC	CASP10-F	TAGGATTGGTCCCCAACAAGA
BID-R	GTAGGTGCGTAGGTTCTGGT	CASP10-R	GAGAAACCCTTTGTCGGGTGG
P21-F	CTCTCCCGAAAAGCAGTCCC	NF- κB-F	GGTGCGGCTCATGTTTACAG
P21-R	GCGAGAACGAGCCAACCTT	NF-κB-R	GATGGCGTCTGATACCACGG

by probiotics in the intestinal microbiota have a protective effect on colon cancer. Probiotics have strong protection in intestinal and colon epithelial cells against toxic components, reactive metabolites, and harmful activities of pathogenic bacteria that are digested and produced in the intestine. Furthermore, probiotics are beneficial by improving the physicochemical conditions of the intestine and decreasing oxidative stress [4,5].

Among the underlying causes of cervical cancer, which is reported as the most common type of cancer among women, are urogenital system infections that lead to the formation of gene mutations [6,7]. In maintaining the homeostasis of a healthy urogenital system, there must be a balance between the host immune system and the urogenital system microbiota. It has been reported that disorders in this balance lead to cervical cancer [8]. An-

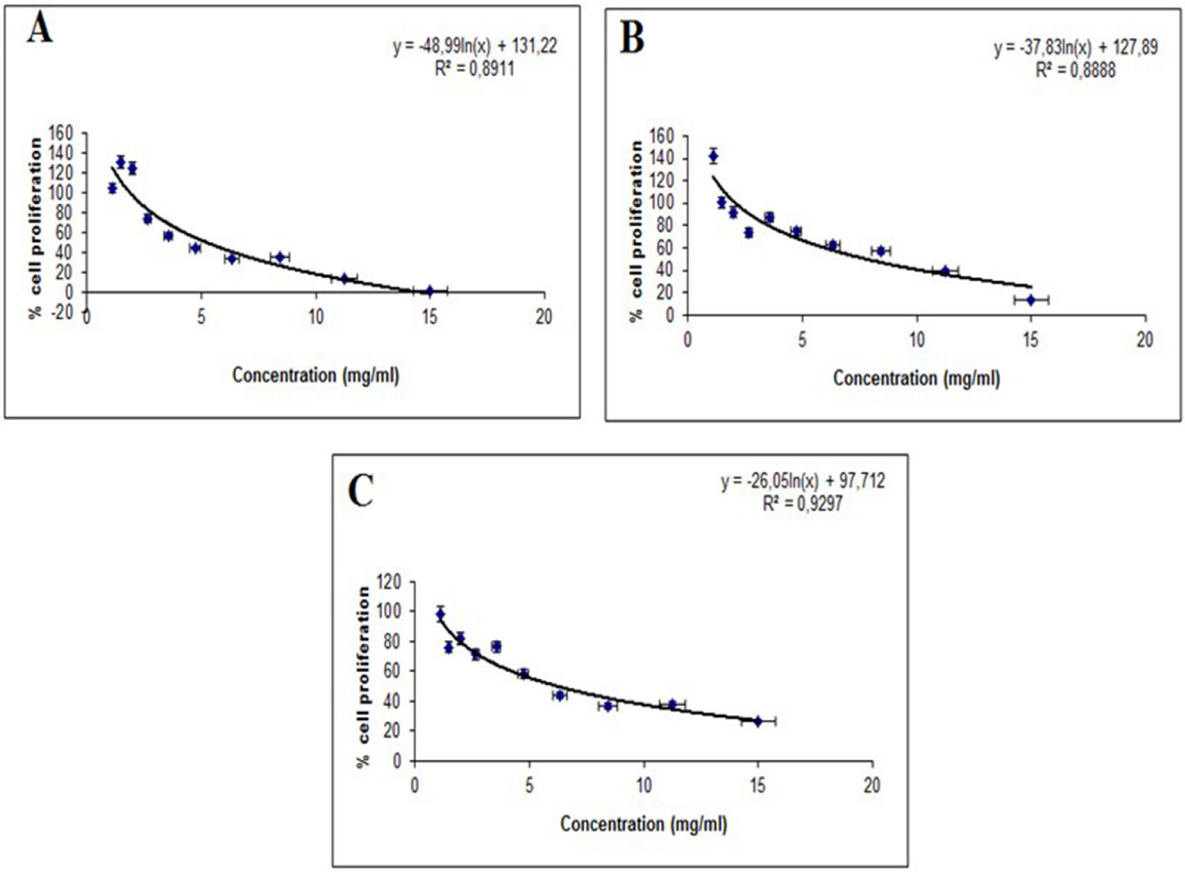

Fig. 1. Graphical representation of the antiproliferative effect microorganisms' metabolites products on MDA-MB-231 cells using XTT cell proliferation kit A- *L. plantarum* AB6-25 B- *L. plantarum* MK55 C- *S. boulardii* T8-3C.

other major risk factor for cervical cancer is human papillomavirus (HPV).E6 inhibits p53, and E7 HPV viral oncogenes, which play a role in the induction of cervical cancer, inhibit the effect of p53 [9]. Probiotics, on the other hand, contribute to the promotion of cell apoptosis by acting at the gene level [8].

Probiotics also play a role in the prevention of breast cancer, which is the most well-known example of hormone-dependent cancer. It is stated that the consumption of probiotics improves the imbalance in the intestinal microbiota and that breast cancer can be treated. In addition, probiotics applied to breast cancer cells caused an increase in some cells responsible for immunity. Probiotics also play a role in promoting certain apoptotic genes by reducing the proliferation of cancer cells. Considering the curative effects of probiotics on cancer cells, as mentioned above, it was necessary to investigate the potential of being an anti-cancer agent. For this purpose, the antiproliferative effects of metabolites obtained from probiotic microorganisms on HCT-116, HeLa, and MDA-MB-231 cell lines were investigated in vitro. In the study, the effects of metabolites on cancer cells at the gene level were also revealed. At the same time, metabolites produced by microorganisms have given important results in bioinformatics studies and have the potential to be anticancer agents.

2. Materials and methods

2.1. Microorganisms

The probiotic properties of *L. plantarum* AB6-25, *L. plantarum* MK-55, and *Saccharomyces cerevisiae boulardii* T8-3C were selected for use in this study. Başyiğit [10] identified *L. plantarum* AB6-25 strain from human feces samples, Kahraman [11] isolated *L. plantarum* MK55 strain from healthy human feces, and Yıldran [12] isolated *S. boulardii* T8-3C yeast from free-running chicken feces samples. *Lactobacillus* strains and *Saccharomyces* were incubated in Man Rogasa Sharpe (MRS, Merck) and medium with sucrose, respectively [13,14].

2.2. Extraction of intracellular metabolites

16–18 h fresh cultures were obtained after activation twice in MRS broth microorganisms stored at -80 °C. The cell contents were prepared as given below:

Cultures were centrifuged at 5000 g for 10 min. After the supernatant was removed, the pellet was dissolved in potassium phosphate buffer (0.1 M, pH 7.5) to approximately 0.1 g/mL. Breakage of the cell walls was achieved with an ultrasonic homogenizer (Optic Ivymen System, CY-500). The cell walls of the samples in ice were broken by applying 75% amplitude (running for 1 min, stopping for 30 s) for 5 min. The adequacy of cell breaking down was determined by examining it under a microscope. After breaking down the cell walls, the samples were centrifuged at 5000 rpm for 10 min. The supernatant was first passed through a 0.45 µm, and then a 0.22 µm membrane filter and stored at +4 °C for later use.

2.3. Quadrupole time-of-flight mass spectrometry (QTOF-LC/MS) analysis

The QTOF-LC/MS analysis of the metabolites was performed at Atatürk University Eastern Anatolia High Technology Application and Research Center. An Agilent QTOF-LC/MS (Agilent 6530, USA) instrument was used. Samples were analyzed with an LC-MC system consisting of a HiP sampler, dual pump, column section, and Q-TOF. Analyses were performed in Dual AJS ESI mode. 10 µl of the sample was injected into the ZORBAX SB-C18 2.1 × 50 mm, 1.8 µm diameter particle packed column (Agilent Technologies, USA) at

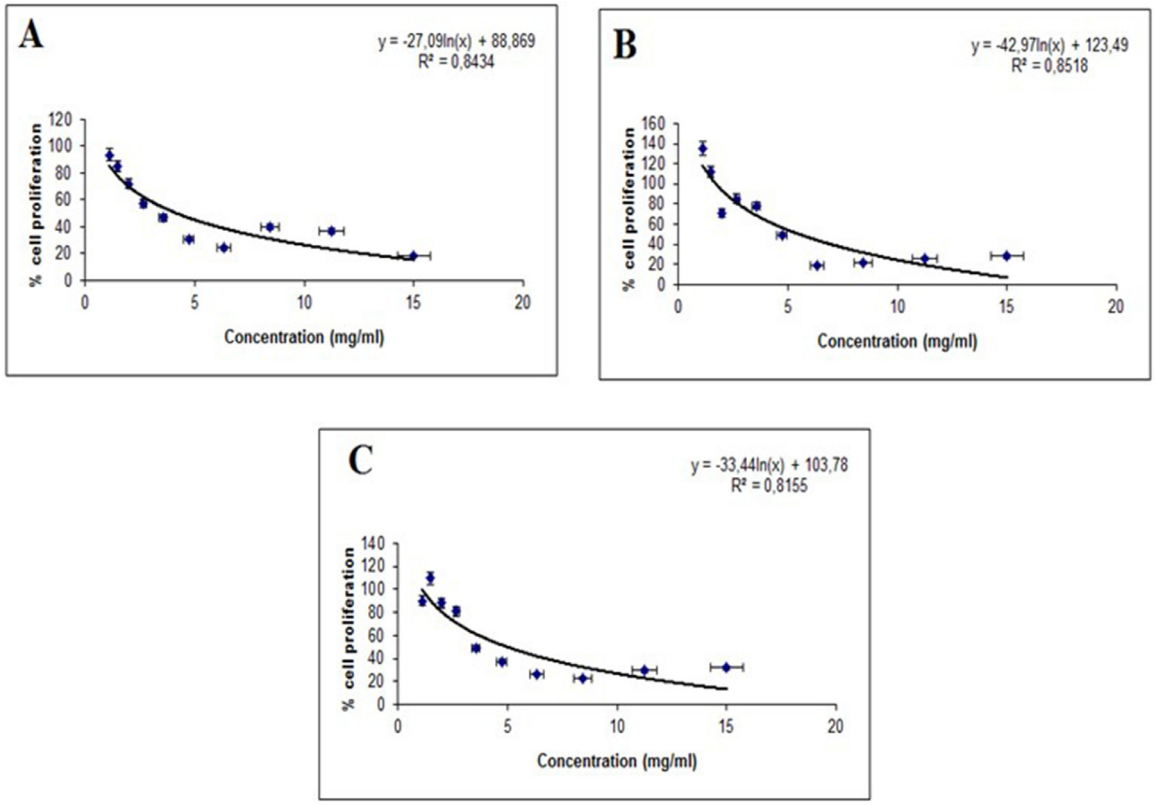

Fig. 2. Graphical representation of the antiproliferative effect microorganisms' metabolites products on HeLa cells using XTT cell proliferation kit A- *L. plantarum* AB6-25 B- *L. plantarum* MK55 C- *S. boulardii* T8-3C.

35 °C. The flow rate in solvent A (0.1% formic acid with H_2O) and solvent B (0.1% formic acid with acetonitrile) was determined as 0.4 ml/min. The gradient started at 5% phase B at 1 min and increased to 95% within 20 min. The gradient returned to initial conditions (5% phase B) within 1 min after reaching 95%. The gradient was held at this solvent ratio for 4 min.

Mass spectrometry was run in AutoMS2 mode between 50 and 2000 m/z. The capillary voltage was set at 3.5 kV, the gas flow at 35 °C, 11 l/min, and the gas pressure at 40 psi. Data was collected by scanning 2 spectra/s in centroid mode. Mass calibration was performed with reference to m/z: 121.05087300 and m/z: 922.00979800 in positive mode, m/z: 68.99575800, m/z: 112.98558700, and m/z: 966.00072500 in negative mode. For the identification of metabolites, the METLIN database was used via the online search engine CEU Mass Mediator [15].

2.4. Cell culture

In the study, colon cancer (HCT-116), cervix cancer (HeLa), breast cancer (MDA-MB-231), and MCF10A healthy breast epithelial cell lines were used. These cell lines were obtained from the Cancer and Stem Cell Laboratory of the Molecular Biology and Genetics Department of Kırşehir Ahi Evran University. The cells were incubated at 37 °C with 5% CO_2 in RPMI medium supplemented with 10% Fetal Bovine Serum and 1% penicillin-streptomycin.

2.5. XTT assay

XTT assay kit (Biological Industries, USA) was used to determine the cytotoxic effect of metabolites on HCT-116, Hela, and MDA-MB-231 cells. 8000 cells were seeded in each well in a 96-well plate. After 24 h of incubation, cells were treated with microorganism metabolites. After 72 h of incubation, the solutions in the XTT kit were added to the cells. Then cell viability was measured by a microplate reader (BIOTEK ELX808, USA) at a 450 nm wavelength. The IC50 value was calculated. Inhibition rates of cells as a result of reading were calculated according to the following formula:

$$\%\,\text{inhibition}: (A_{450}\text{nm test} - A_{450}\text{nm control}/A_{450}\text{nm control}) \times 100$$

2.6. 3D cell culture

Cells were harvested and approximately 10^4 cells/mL were seeded dropwise on a sterile Petri dish cover [16]. The cells were incubated for 48 h at 37 °C with 5% CO_2. After the 3D structure was formed different concentrations of cell extracts (0.4, 1, 4, and 10%) were applied to the cell lines. The method suggested by Qu et al. [17] was used in the development of MCF10A healthy breast epithelial cells in 3D.

2.7. Wound healing assay

1.5×10^5 cells were seeded in 6-well plates and incubated at 37 °C with 5% CO_2 for 48 h. When the cells were 80% confluent at the end of the incubation, the cells were wounded with a 20–200 µL pipette tip [18]. Then 4 mL of fresh medium and 1 mL of metabolites were added. The wound closure was monitored and imaged using an inverted microscope (BAB, Türkiye). Wound closure rates were evaluated using the ImageJ program.

2.8. Invasion assay

Cell culture inserts were placed in 24-well plates and 100 µL of a previously prepared stock of 1:10 matrigel was added. The

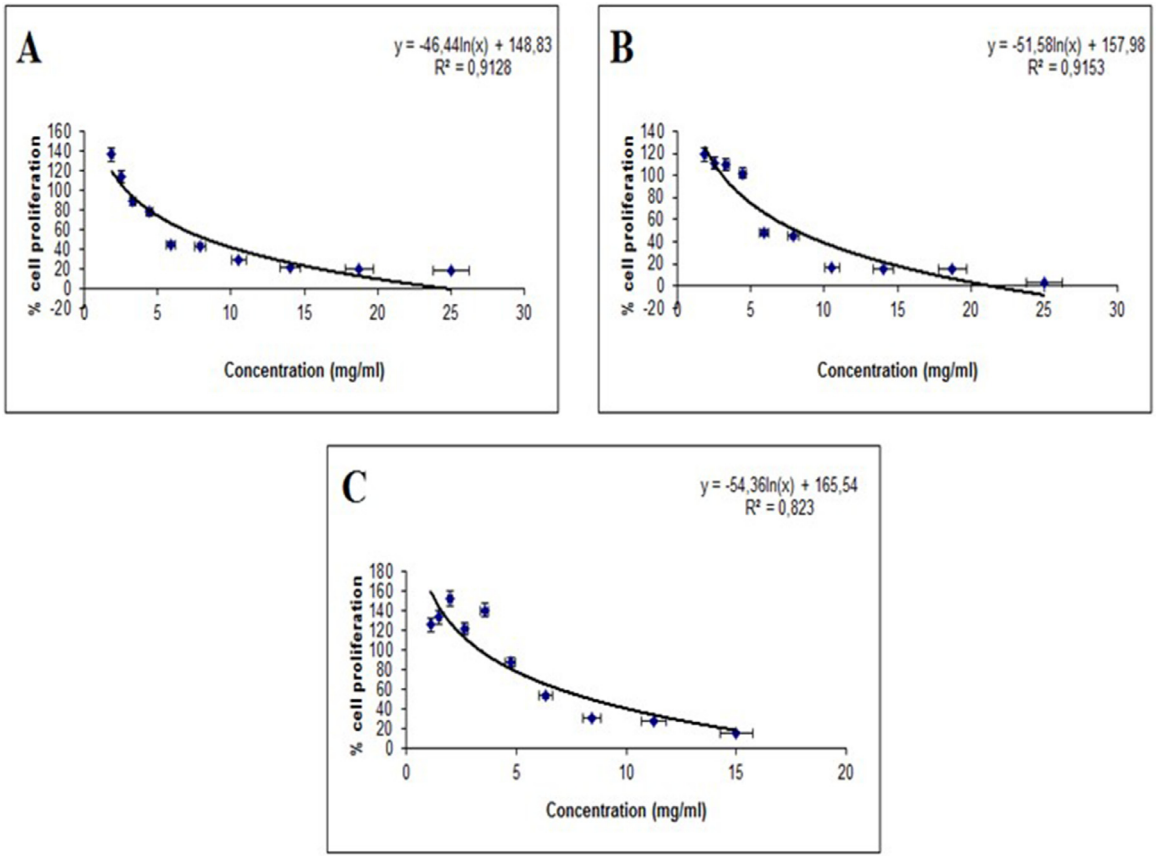

Fig. 3. Graphical representation of the antiproliferative effect microorganisms' metabolites products on HCT-116 cells using XTT cell proliferation kit A- *L. plantarum* AB6-25 B- *L. plantarum* MK55 C- *S. boulardii* T8-3C.

plate was incubated for 48 h at 37 °C to form a gel consistency. After the desired structure was formed in the matrigel, RPMI-1640 medium containing fetal bovine serum (FBS) was added to the wells. Serum-free RPMI-1640 medium was added to the matrigel-containing insert and approximately 106 cells were inoculated. This medium containing cancer cells were placed in wells containing medium containing serum. The plate was then incubated at 37 °C for 48 h. After incubation, the cells were treated with 10% formaldehyde for 10 min. Then cells are stained with Giemsa [19].

2.9. Genetics experiments

2.9.1. Total RNA isolation and cDNA synthesi

Cells cultured in 2D and 3D were harvested and total RNA isolation was performed according to the protocol using the High Pure RNA Isolation Kit/Roche kit. The cDNA synthesis was performed using the WizScript ™ cDNA Synthesis Kit (High Capacity). The reaction was carried out using a thermal cycler. Finally, real-time qPCR (RT-qPCR) was performed to determine the change in gene levels. In total, 20 genes associated with apoptosis were used in the analysis. Primers' information was indicated in the table below (Table 1). The Real-Time qPCR reaction was performed on the Applied Biosystems™ 7500 Fast Real-Time PCR instrument.

2.9.2. Western blotting analysis

According to the gene expression results CASP3 protein was investigated after three microorganisms' metabolites were treated to cells. First of all protein isolation was performed. Protein concentration was determined using the Qubit® 3.0 Fluorometer instrument (Thermo Fisher Scientific, Cat. no: Q33216, USA) according to the manufacturer's instructions using the Qubit® Protein Assay Kits (Thermo Fisher Scientific, Cat. no: Q33211, USA).

Protein samples were mixed with 4X NuPAGE LDS Sample Buffer, and 10X NuPAGE Sample Reducing Agent and distilled water and incubated at 70 °C for 10 min and then kept on ice for 2 min. Samples were then loaded into each well for SDS-PAGE. Following electrophoresis, the protein samples were transferred to a nitrocellulose membrane and incubated for 1 h in a blocking solution (5% BSA-PBST) prepared with PBS (PBS-T) solution containing 5% BSA (Bovine Serum Albumin) and 0.1% Tween-20. After incubation, the membrane was washed three times in PBST and incubated with primary antibodies (CASP3 and β-Actin) overnight at +4 °C. At the end of incubation with primary antibodies, three washes were made with PBST again and incubated with secondary antibodies (Goat-anti-rabbit IgG (H+L), HRP conjugate) for 1 h. At the end of the process, gel images were captured using a luminometer, and bands were observed. At the end of the process, gel images were captured using a luminometer and bands were observed.

2.10. Molecular docking approach

2.10.1. Protein and ligand preparation

The three-dimensional structures of the proteins accessed were provided from the RCSB PDB protein database in pdb. file format [20] (https://www.rcsb.org/). Three-dimensional structures of metabolites determined as a result of QTOF-LC/MS analysis

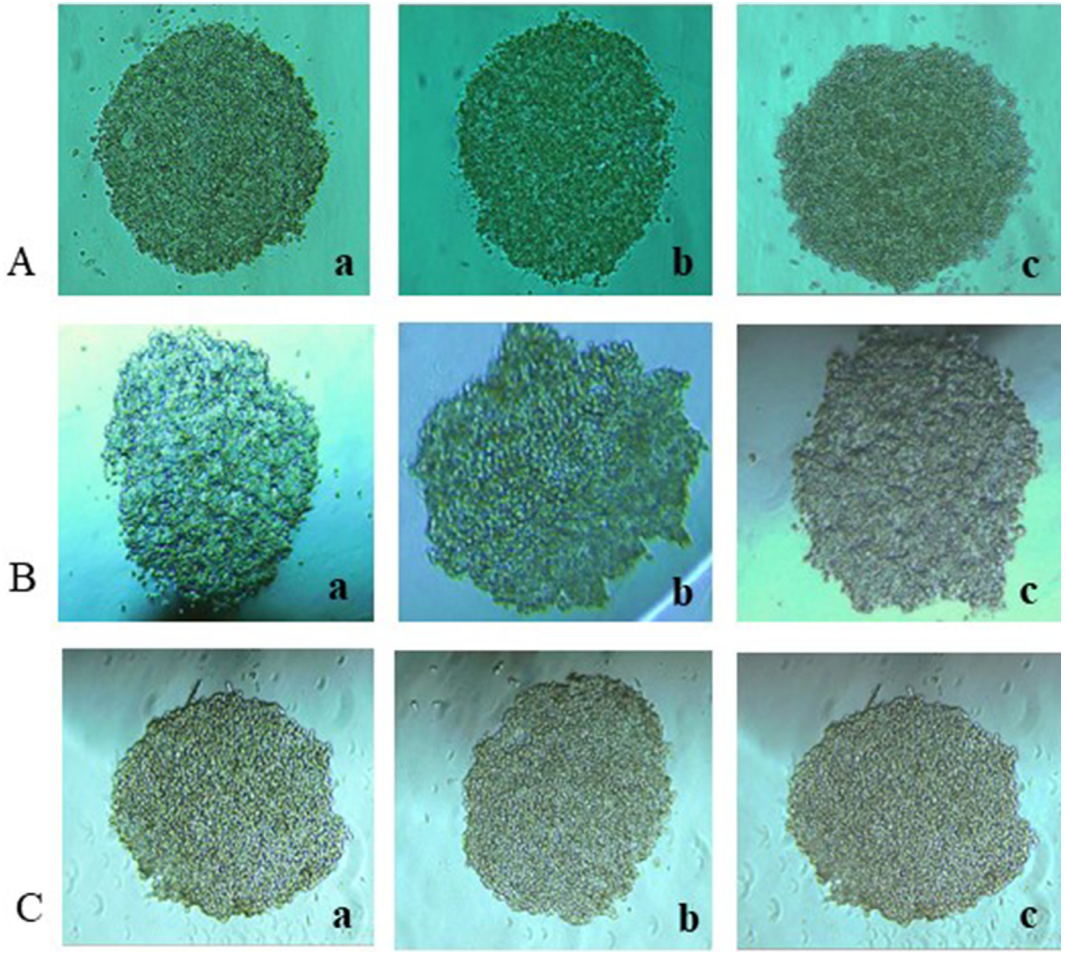

Fig. 4. (A) HCT-116 cells control a. 0 h, b. 24 h, c. 48 h (B) HeLa cells control 0 h b. 24 h hour c. 48 h hour (C) MDA-MB-231 cells control a. 0 h, b. 24 h, c. 48 h.

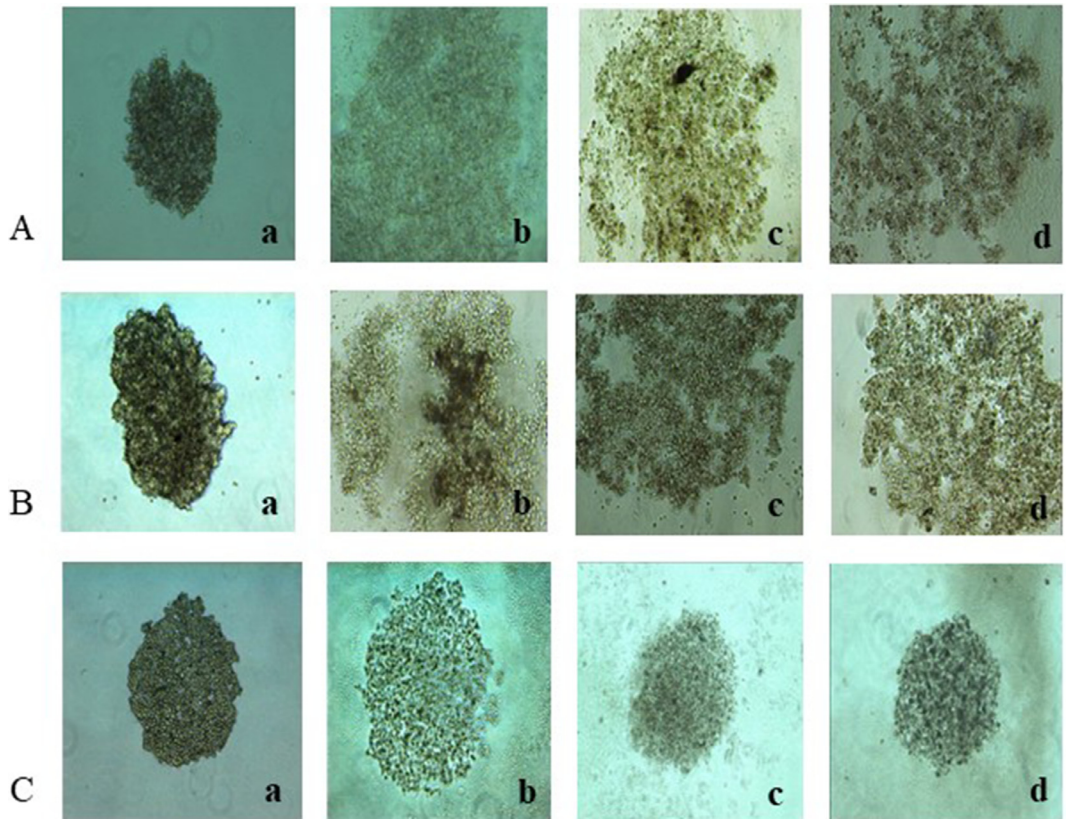

Fig. 5. (A) HCT-116 cells a-control b-AB6-25 24 h c-MK55 24 h d-T8-3C 24 h (B) HeLa cells a-control b-AB6-25 24 h c-MK55 24 h d-T8-3C 24 h (C) MDA-MB-231 cells a-control b-AB6-25 48 h c-MK55 48 h d-T8-3C 48 h.

were obtained from the PubChem database in pdb. file format [21] (https://pubchem.ncbi.nlm.nih.gov/). Molecular docking calculations were obtained using Autodock Vina. Firstly, the water in the protein structure was removed and polar hydrogen bonds were added. Kollman and Gasteiger charges were distributed over the entire structure. Torsion roots and torsion numbers of the ligand molecule were determined. Both the protein and the ligand were saved in PDBQT format. Ligand and protein structures were brought together, their borders were enclosed in a box, and grid parameters were entered. At the last stage, the necessary command was entered into the Windows command system to start the calculation process and the binding energies (kcal/mol) were determined [22]. The interactions between the molecules and the hydrogen (H)-bonds were visualized with the Molegro Molecular Viewer program (http://molexus.io/molegro-molecular-viewer/).

2.11. Molecular dynamics (MD) simulation approach

Simulation of the ligand and protein complex was performed using WebGro application [23]. MD simulation was performed for 50 ns to check the stability between the ligand and protein complex [24–28].

2.12. Statistical analysis

All *in vitro* experiments were performed in two parallels. The data was statistically evaluated using the Student *t* test.

3. Results and discussion

3.1. XTT assay

Table 2 shows the IC50 values and inhibition percentages of bacterial metabolites. In HeLa and MDA-MB-231 cancer cell lines, AB6-25 was found to be the most effective strain. On HCT-116 cells, MK55 had the most cytotoxic effect. Two *L. plantarum* strains were shown to have stronger anticarcinogenic effects than *S. boulardii* when examined in this way.

Cytotoxic effects of microorganisms' metabolites on cancer cells were determined (Figs. 1–3).

Similar to this study, Bharti et al. [29] found that the cell content of *L. acidophilus* KP942831 and *L. plantarum* KP894100 provided a strong inhibition of 80% and 98%, respectively, on U87 cells. The cell content of *L. acidophilus* KP942831 and *L. plantarum* KP894100 inhibited cell proliferation by 97% and 98%, respectively,

Table 2
IC_{50} values and inhibition percentages of microorganisms' metabolites.

Strain	Cytotoxicity	HCT-116	HeLa	MDA-MB-231
L. plantarum AB6-25	IC_{50} (mg/ml)	5.55	3.5	3.9
	Inhibition (%)	39	91	80
L. plantarum MK55	IC_{50} (mg/ml)	5.0	4.5	5.13
	Inhibition (%)	69	52	68
S. boulardii T8-3C	IC_{50}(mg/ml)	6.6	4.0	4.48
	Inhibition (%)	2.90	75	77

in MCF-7 cells. In another study, Bibalan et al. [30] found that three of the 13 *Lactobacillus* strains obtained from the feces of healthy individuals showed strong antiproliferative effects against the HT-29 cells. It was determined that the remaining 10 strains inhibited the proliferation of HT-29 cells by less than 20% or showed no antiproliferative effect. Sambrani et al. [31] found that the supernatant obtained from *S. cerevisiae* killed 75% of HT-29 cells within 48 h. On the other hand, in this study, while the cell content of *S. boulardii* T8-3C showed weak inhibition in HCT-116 cells, it provided better inhibition in HeLa and MDA-MB-231 cells.

3.2. 3D cell culture

Cellular integrity was intact as expected in the 3D HCT-116, HeLa, and MDA-MB-231 cells (Fig. 4). When AB6-25, MK55 and T8-3C cell contents were applied to the HCT-116 and HeLa cells, the spherical cell structure was dispersed within 24 (Fig. 5A, B). Compared to the effect of the other two bacterial cell contents, the structure remained more intact in the cell line treated with T8-3C cell contents. When the microorganism cell contents were applied to MDA-MB-231 cells, the spherical structure did not change within 24 h, while the outer parts of the 3D structure began to disintegrate after 48 h (Fig. 5C). This showed that the MDA-MB-231 breast cancer cell line was more resistant to microorganisms' metabolites.

Similar to this study, Lee et al. [32] applied different concentrations (6%, 12.5% and 25%) of *L. fermentum* supernatant to different 3D colon cancer cell lines (DLD-1, HT-29, WiDr). An increasing concentration of *L. fermentum* supernatant proportionally decreased cell viability within 48 h. At the end of the study, the researchers emphasized that the data obtained is an important preclinical study in cancer treatment. In this study, microorganism cell contents applied to three cell lines at different concentrations (0.4, 1, 4 and 10%) caused significant disruption in the 3D structure at the highest concentration.

In the study, irinotecan applied at the lowest concentration to the HCT-116 cells caused corruption from the edges of the 3D structure after 48 h. On the other hand, irinotecan brought the 3D structure together instead of corrupting it at IC_{50}x2 fold, IC_{50}x3 fold, and IC_{50}x5 fold concentrations. The highest concentration of irinotecan (IC50 $\times$ 10 fold) applied to the HCT-116 cells caused the complete corruption of the 3D structure within 24 h.

There was no significant difference between the lowest IC_{50} and the highest IC_{50}x10 concentrations of irinotecan applied to the HeLa cells. As a result, the effect of irinotecan on the 3D HeLa cells was weak compared to the contents of the microorganism cell.

MDA-MB-231 cells Irinotecan applied at the lowest concentration destroyed the inner parts of the 3D structure within 48 h. On the other hand irinotecan applied at IC50 $\times$ 3 concentration significantly dispersed the 3D structure within 24 h compared to the other two cell lines. Accordingly, MDA-MB-231 cells were more sensitive to irinotecan than HCT-116 and HeLa cells.

Lim and Park [33] applied different concentrations (0, 1.25, 2.5, 3.75, and 5 M) of irinotecan to the 3D HCT-116 and U87 cells for 5 days. With the increase in concentration, the 3D structure started to shrink.

In the study, the 3D structure was not formed in the control group of MCF10A cells after 48 h of incubation. For this reason, cells were incubated for 72 h and 10 days. There was no significant change in the shape of the cells during either of the incuba-

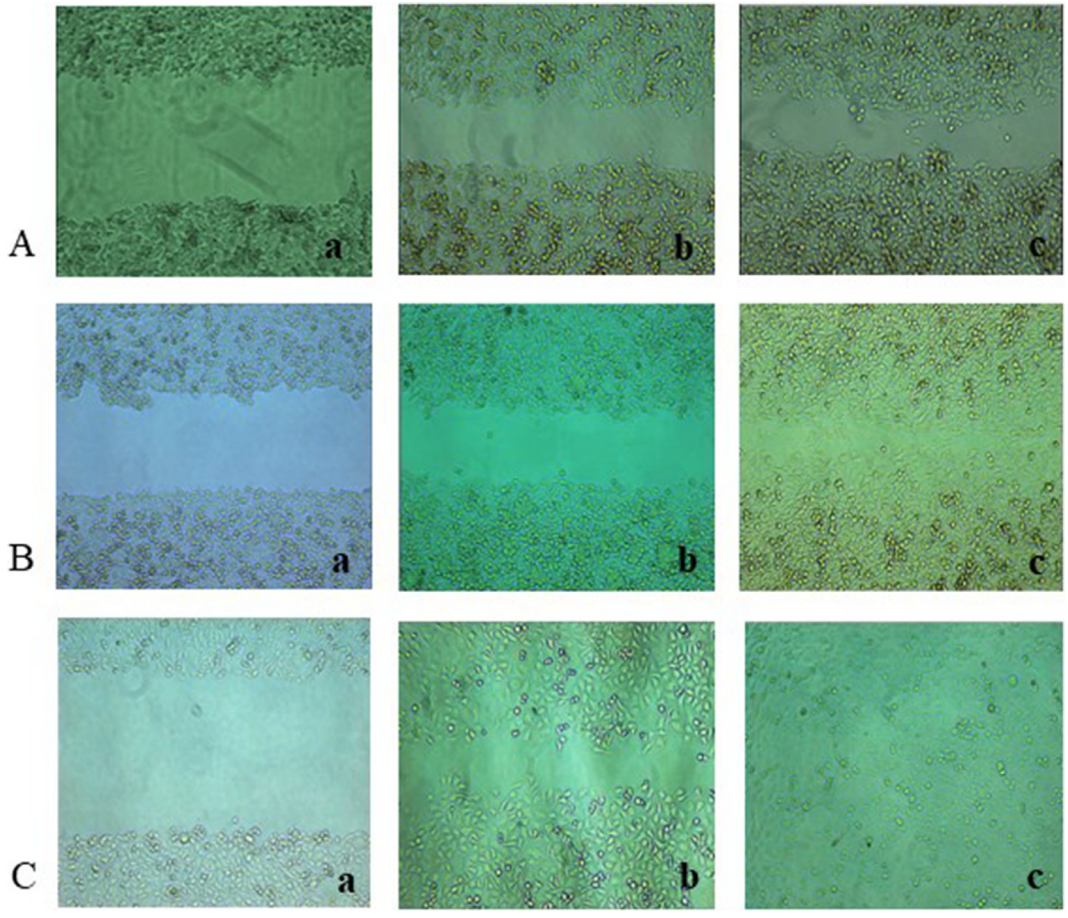

Fig. 6. (A) HCT-116 cells control a-0 h b-24 h c-48 h (B) HeLa cells control a-0 h b-24 h c-48 h (C) MDA-MB-231 cells control a-0 h b-24 h c-48.

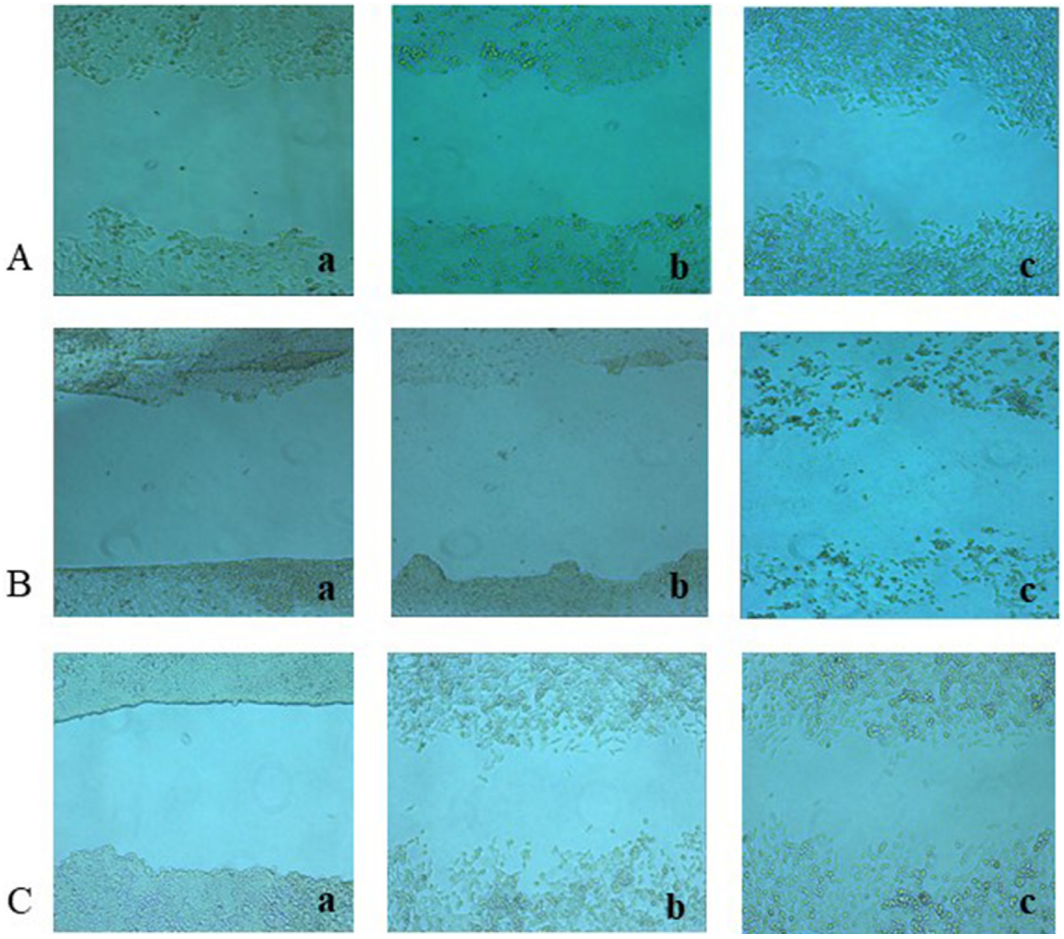

Fig. 7. (A) AB6-25 treated HCT-116 cells a-0 h b-24 h c-48 h (B) MK55 treated HCT-116 cells a-0 h b-24 h c-48 h (C) T8-3C treated HCT-116 cells a-0 h b-24 h c-48 h.

tion periods. There was no difference in MCF10A cells treated with the three microorganism cell contents. This result suggests that if the probiotic microorganisms used in the study were applied therapeutically to cancer cells, they would not have an adverse effect on normal cells.

3.3. Wound healing and invasion assay

In HCT-116 cells, the wound closed 86% within 48 h in the control group. The closure rate in HeLa cells and MDA-MB-231 cells against HCT-116 cells was 91% and 99%, respectively (Fig. 6). In HCT-116 cells treated with AB6-25 the wound was closed by 45% within 48 h, whereas in cells treated with MK55, it was closed by 34%. In HCT-116 cells treated with T8-3C the wound patency was closed by 77% within 48 h (Fig. 7). This result showed that T8-3C inhibited migration less than bacteria.

Shang et al. [34] found that while the wound on the CT26 cells in the control group closed 60%, the probiotic mixture including *L. plantarum* closed the wound by 40%. In this study, untreated HCT-116 cells closed by 86%, while the wound opening in AB6-25 and MK55-treated cells decreased to 45% and 34%, respectively. In contrast, Khoury et al. [35] found that no change was observed in cells treated with kefir in colon cancer (Caco-2 and HT-29) cell lines compared to the control group. Wound healing was 10% in HeLa cells treated with AB6-25 (Fig. 8A), while 5% in MK55 (Fig. 8B). In contrast, T8-3C increased the wound by 4% (Fig. 8C). Somaida et al. [36] reported that in the control group of HeLa cells, the wound was healed by 96% within 24 h, and when the extract obtained from four different plants was treated, the wound was healed by 38, 36, 27, and 11.5%. When compared with this study, the microorganisms showed that they were more effective in inhibiting migration in HeLa cells than plant extracts.

Wound healing was 59% in MDA-MB-231 cells treated with AB6-25. In contrast, the wound expanded by 4% in MDA-MB-231 cells treated with MK55 (Fig. 9A, B). The wound healed by 65% after treatment with T8-3C in the MDA-MB-231 cells (Fig. 9C). As a result, T8-3C was found to be more ineffective on cell migration in MDA-MB-231 cells than in bacteria.

Wang et al. [37] reported that the wound healing was 100% in the control group in MDA-MB-231 cells, while the wound healed by 40% within 48 h in the group treated with a commercially available herbal mixture consisting of eight natural products. Sun et al. [38] found that 100% of the wound was healed in MDA-MB-231 cells, while it prevented the closure of the wound opening by 25% in cells treated with emodin, a plant extract. Contrary to these studies, Khoury et al. [35] stated that kefir did not significantly affect the migration ability of MCF-7 and MDA-MB-231 cells.

In the study, the wound healed by 53% within 48 h in MCF10A cells. Wound closure was 14% in MCF10A cells treated with AB6-25, whereas MK55 and T8-3C had no effect on wound closure. Accordingly, AB6-25 was found to be the most effective strain in wound healing in healthy MCF10A cells.

As a result of the invasion assay, it was observed that the cytoplasmic structure and nuclei of the cells in the microorganism control group had a significant density (Fig. 10I). A significant decrease in cell density was detected in cells treated with AB6-25, MK55, and T8-3C. In addition, it was observed that the cytoplasmic structures of the cells disappeared and the nuclei became smaller

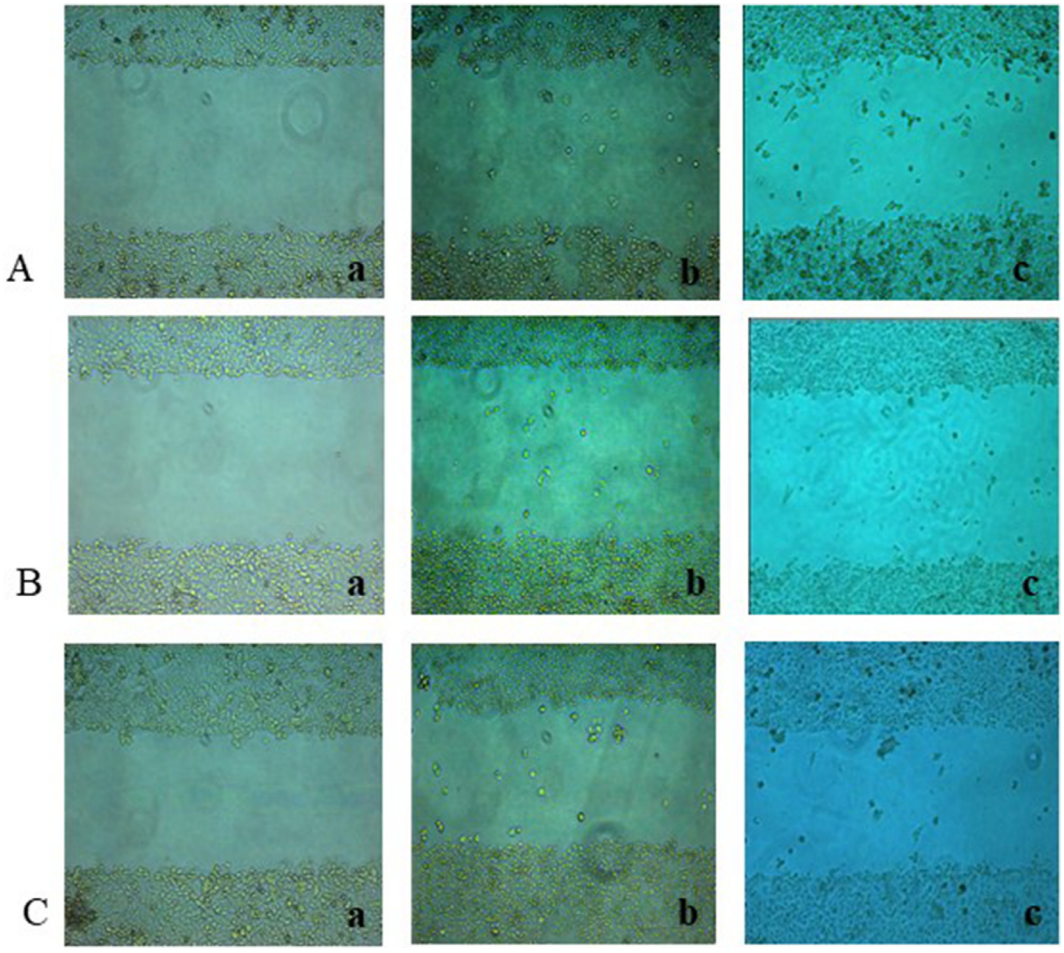

Fig. 8. (A) AB6-25 treated HeLa cells a-0 h b-24 h c-48 h (B) MK55 treated HeLa cells a-0 h b-24 h c-48 h (C) T8-3C treated HeLa cells a-0 h b-24 h c-48 h.

(Fig. 10II–IV). Similarly, Shang et al. [34] reported decreased cell density in CT26 cells treated with a probiotic mixture including *L. plantarum* compared to control.

The results of migration and invasion assays show that microorganisms' cell contents prevent metastasis in cancer cells. These results were also validated at the gene level.

3.4. Gene expression analysis

The greatest change in gene expression level with the treatment of microorganisms was in HeLa cells. While MK55 caused resistance in 3D HeLa cells to different metabolic pathways in general, it was the most effective strain in 2D HeLa cells (Fig. 11). On the other hand, AB6-25 increased the expression of genes promoting cell apoptosis at a higher level in 3D HeLa cells (Fig. 12). In contrast, T8-3C was more effective on genes in 2D enhanced HeLa cells (Fig. 13).

Lee et al. [32] *L. fermentum* supernatant caused a significant increase in the expression of *BAX, BAK, BCL-XL,* and *NOXA* genes in different 3D colon cancer cells (DLD-1, HT-29, WiDr). It was also found that NF-kB activity was inhibited. Contrary to this, Nouri et al. [39] reported that *L. crispatus* and *L. rhamnosus* supernatants decreased the expression level of *CASP3* in HCT-116 and HeLa cells. In Pakbin et al. [40], it was stated that the *S. boulardii* supernatant decreased the expression of the *BIRC5* gene in gastric cancer cells and induced apoptosis. On the other hand, Venkatachalam and Nadumane [41] reported that secondary metabolites obtained from *Penicillium rubens* increased *BAX* gene expression in HepG2, HeLa, and MCF-7 cells and decreased BCL-2 gene expression. In addition, there was an increase in the expression of *CASP3, CASP7, CASP10,* and *p53*.

3.5. Western blot analyses

Gene expression analysis results showed that the CASP3 gene was expressed at the highest level in HeLa cells. The effect of microorganisms on the increase in the expression of CASP3 protein was examined by western blot (Fig. 14). While CASP3 formed a more prominent band in the 2D cells treated with AB6-25, MK55, and T8-3C, a thinner band was observed in the 3D cells. This is due to the fact that the *CASP3* gene is expressed at a higher level in 2D HeLa cells than in 3D cells. Wan et al. [42] showed the effect of *L. delbrueckii* supernatant on the increase in the expression of *CASP3* and the decrease in the expression of the antiapoptotic *BCL-2* gene in SW620 cells. In an *in vivo* study by Gamallat et al. [43], a decrease in *BCL-2* expression and an increase in *BAX, CASP3,* and *p53* expression were visualized by western blot after treatment with *L. rhamnosus* GG CGMCC (LGG). In another study, Riaz Rajoka et al. [8] observed that an increase in the expression of *BAX*, BAD, CASP3, CASP8, and CASP9 proteins in HeLa cells treated with *L. casei* and *L. paracasei* supernatants was observed with significant banding, while the expression level of BCL-2 protein produced very weak banding.

3.6. QTOF-LC/MS

In the study, only 74 metabolites of the *L. plantarum* AB6-25 strain, 16 of the *L. plantarum* MK55 strain, and 88 metabolites of

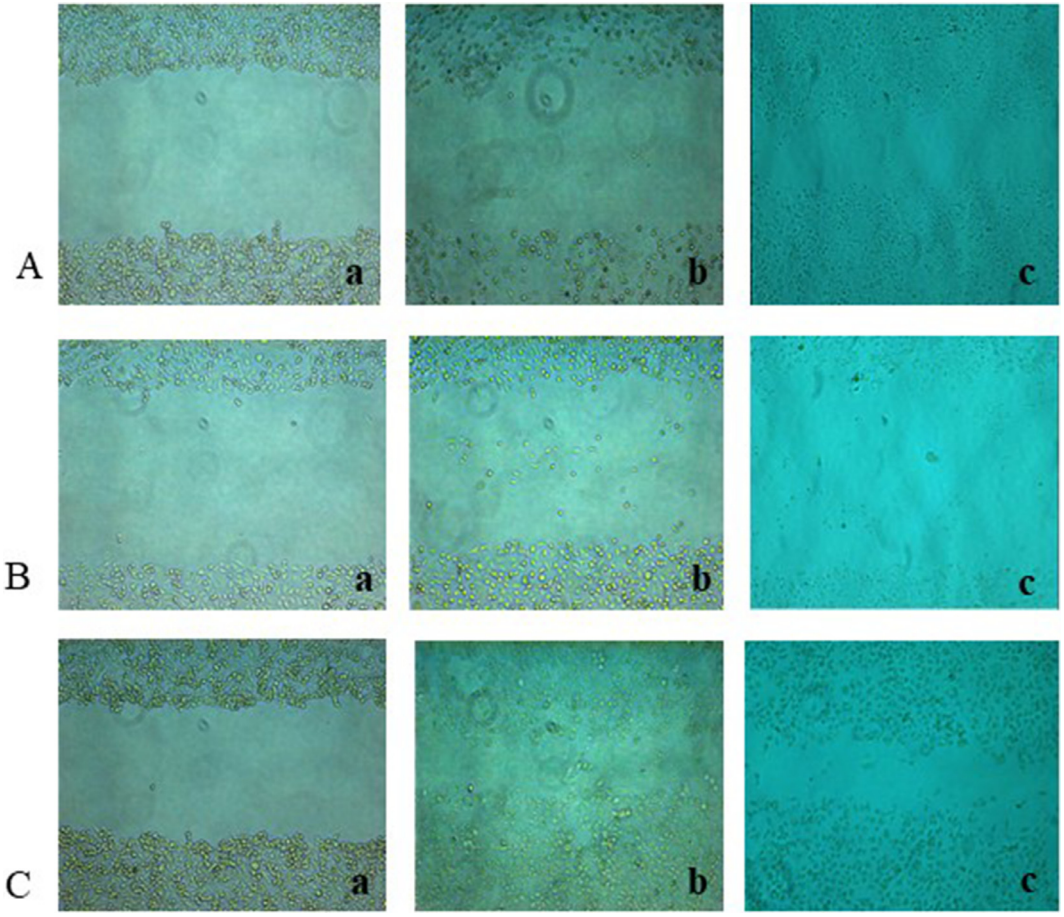

Fig. 9. (A) AB6-25 treated MDA-MB-231 cells a-0 h b-24 h c-48 h (B) MK55 treated MDA-MB-231 cells a-0 h b-24 h c-48 h (C) T8-3C treated MDA-MB-231 cells a-0 h b-24 h c-48 h.

the *S. boulardii* T8-3C strain were determined, out of 248 compounds detected (Figs. 15–17).

In vitro studies on the procaspase-activating component (PAC-1), which was detected only in *L. plantarum* AB5-25 as a result of QTOF-LC/MS, were found to activate the proapoptotic gene PROCASP3 [44]. Regarding this, Lucas et al. [45] reported an increase in the CASP3 activity of lymphoma cancer cells after treatment with PAC-1.

Studies show that probiotic yeasts and their metabolites have anticancer effects. However, there is limited research on the identification of metabolites from probiotic yeasts, including *S. bouilardii*. In the study by Yıldıran [12] it was determined that *S. bouilardii* T8-3C produced tartaric acid, oxalic acid, malic acid, lactic acid, acetic acid, citric acid, and propionic acid in the organic acid determination made by HPLC. In the analysis of volatile components and aroma substances by GC/MS, it was determined that T8-3C produced butyric acid, benzaldehyde, 3-methylbutanal, acetone, ethyl alcohol, and acetaldehyde as volatile components. As a consequence of this research, organic acids, tripeptides, purine compounds, disaccharides, organosulfur heterocyclic compounds, lipids, and lipid-like organic compounds of T8-3C were identified using QTOF-LC/MS data.

Two important metabolites found to be produced only by T8-3C in the study are MY-5445, known as a phosphodiesterase type-5 inhibitor, and EX-527, an inhibitor of the SIRT1 enzyme, which plays a role in cancer development. In a study by Wu [46], MY-5445 strengthened drug-induced apoptosis by inhibiting the function of ABCG2, which is overexpressed in multidrug-resistant cancer cells. Thus, it has been stated that cancer cells become sensitive to the drug again. Solomon et al. [47] reported that the catalytic activity of SIRT1 was inhibited by EX-527 in several cancer cell lines, including MCF-7 cells.

3.7. Molecular docking study

For the molecular docking study, *BAX*, BCL-2, BRAF, CASP3, CASP8, NF-κB and p53 proteins with the highest expression levels as a result of the gene expression study were used.

In the study, it was observed that H bonds did not form between the BRAF with the highest binding energy and istamycin C1. It was determined that two H bonds were formed between CASP3, which has the lowest binding energy, and thiodicarb, in the regions of Ile265 and Ser267 amino acids. Therefore, in molecular docking studies, in addition to the high binding affinity of two molecules, the number of H-bonds formed between them also reveals the strength of the docking.

In the study, ligands with the highest binding energy and a high number of H bonds with each other were selected as candidates with a strong potential to be anticancer active agents. Between BCL-2 and PAC-1, which provides these properties, a total of six H bonds and a binding energy of -7.25 kcal/mol were formed from the regions of Ala146, Phe147, Phe148, Phe150, Tyr308, and Val145 amino acids. The docking results of ligands with high affinity for the *BAX* protein are given in Table 3.

The interaction between *BAX* protein and istamycin C1 ligand, where the strongest bond energy occurs, is given in Fig. 18.

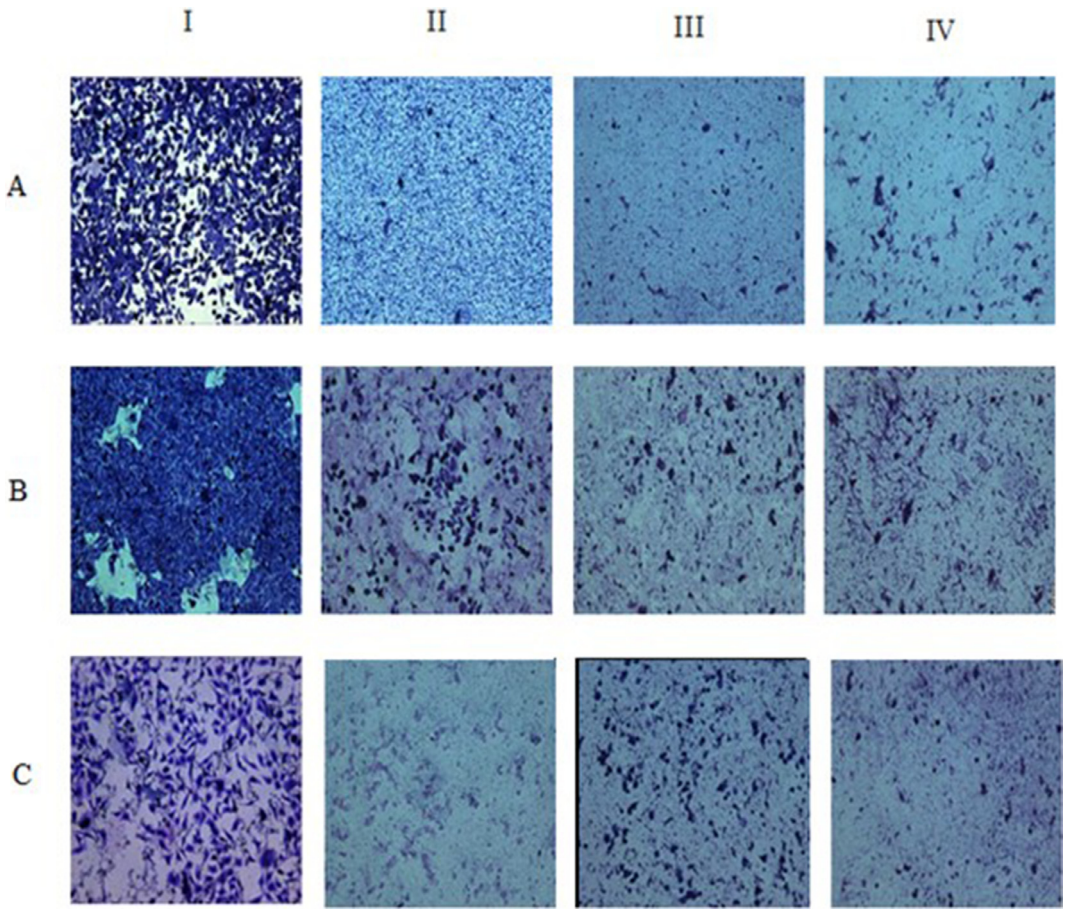

Fig. 10. (A) HCT-116 cells (I) control, (II) treatment with AB6-25, (III) treatment with MK55, (IV) treatment with T8-3C (B) HeLa cells (I) control (II) AB6-25 (III) treatment with MK55, (IV) treatment with T8-3C (C) MDA-MB-231 cells (I) control (II) treatment with AB6-25 (III) treatment with MK55 (IV) treatment with T8-3C.

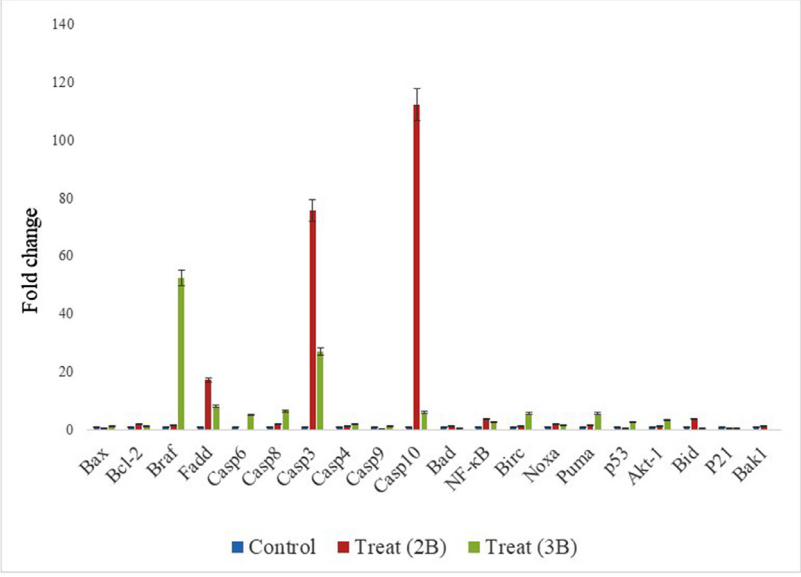

Fig. 11. Expression in 2D and 3D HeLa cells control and genes after treatment with MK55.

The results obtained with irinotecan were similar to the molecular coupling study with microorganism metabolites (Table 4).

It was observed that plant-derived metabolites were more frequently investigated while there were limited studies on the use of probiotics in molecular docking studies in the literature. Sampath et al. [48] investigated the potential of 1,8-Cineole from the plant Callistemon citrinus to be an anticancer active agent in the skin cancer cell line. The binding energies between 1.8-Cineole and BCL-2 and 1.8-Cineole and the PARP1 receptor, a protein involved in cell apoptosis, were determined as -4.99 kcal/mol and -5.60 kcal/mol, respectively. In another study by Ata et al. [49], the interaction of five metabolites of Annona muricata with BCL-

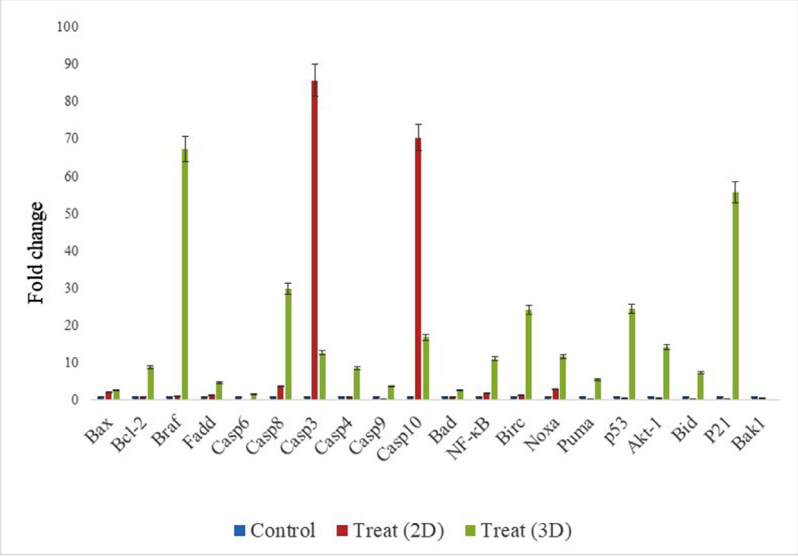

Fig. 12. Expression in 2D and 3D HeLa cells control and genes after treatment with AB6-25.

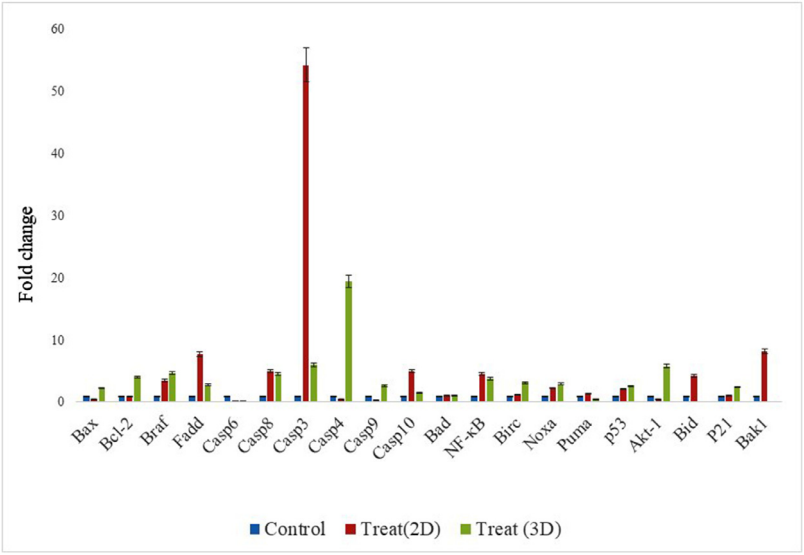

Fig. 13. Expression in 2D and 3D HeLa cells control and genes after treatment with T8-3C.

Table 3
BAX protein and drug candidate molecules (ligands) molecular docking results.

Ligands	Binding Energy (kcal/mol)	Number of H Bonds	H Bonds Position
Istamycin C1	-8.23	5	Pro88 Leu185 Trp188 Lys189 Thr182
N-acryloylglycine	-8.15	4	Ile187 Thr186 Trp188 Val91
Pycnolide	-8.08	3	Ala183 Ile187 Thr186
Quinoline-3-carboxamides	-8.15	4	Ile187 Thr186 Trp188 Val91

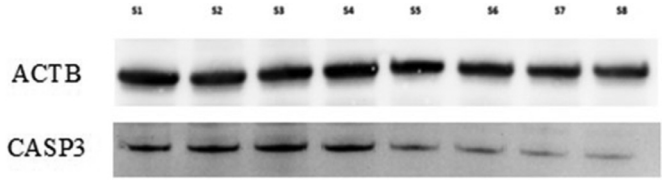

Fig. 14. CASP3 expression level S1: Control (2D) S2: AB6-25 (2D) S3:MK55 (2D) S4: T8-3C (2D) S5: Control (3D) S6:AB6-25 (3D) S7: MK55 (3D) S8: T8-3C (3D).

2, BAD, and AKT1 proteins was investigated. At the end of the study, isoquercetin, which was determined as the most effective metabolite of A. muricata, formed -8.8 kcal/mol,-10.0 kcal/mol, and -7.2 kcal/mol of binding energy with BCL-2, AKT1, and BAD proteins, respectively. The binding energy of abemaciclib anticancer drug used as the positive control group with BCL-2, AKT1 and BAD proteins was found to be -8.0 kcal/mol, -9.4 kcal/mol and -6.9 kcal/mol, respectively.

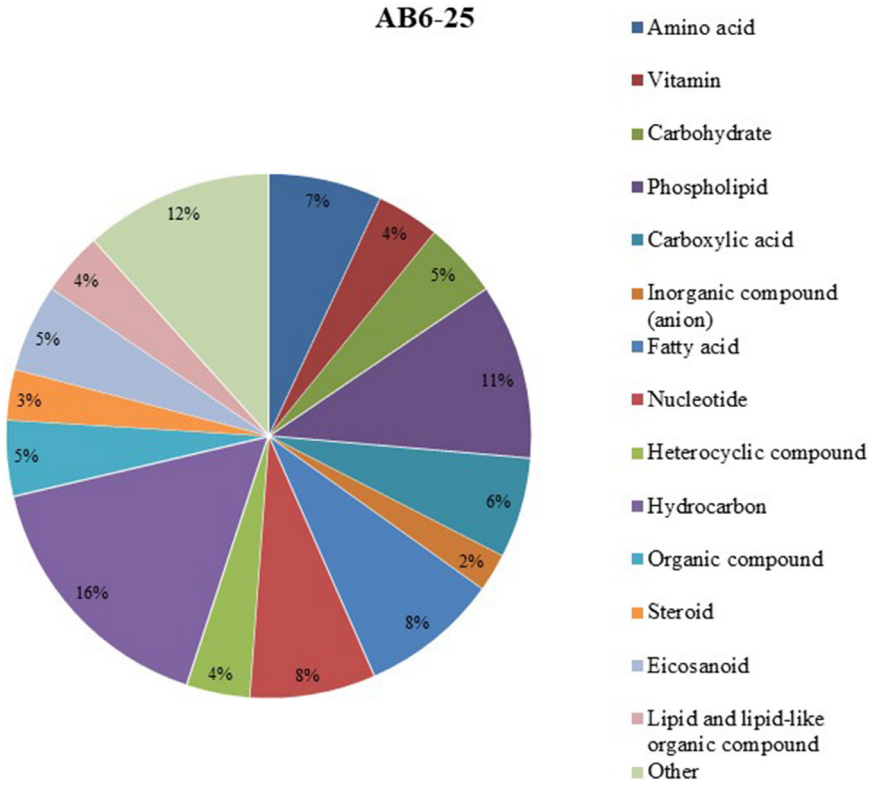

Fig. 15. Distribution of components of *L. plantarum* AB6-25 as a result of QTOF-LC/MS.

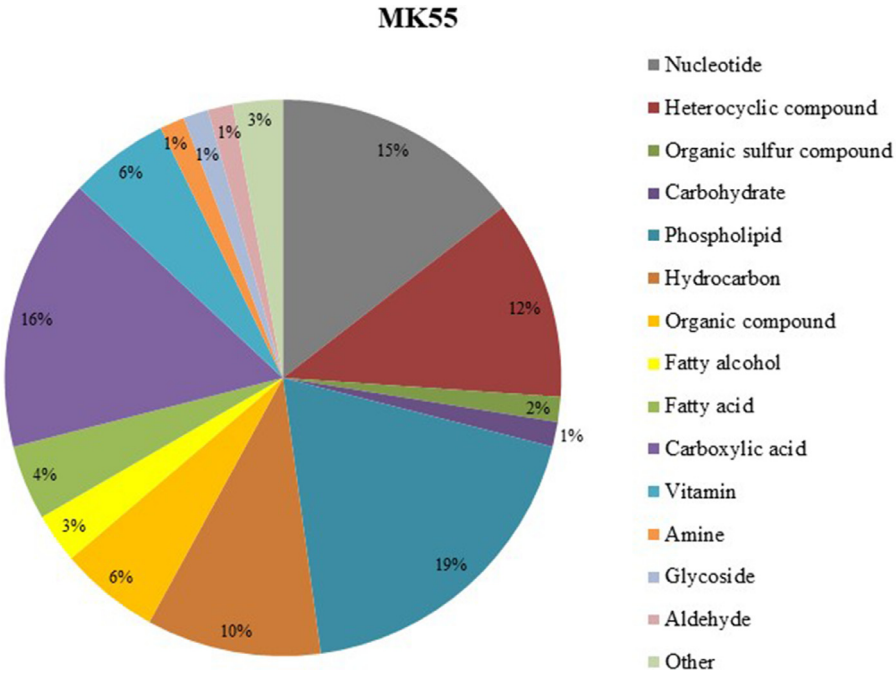

Fig. 16. Distribution of components of *L. plantarum* MK55 as a result of QTOF-LC/MS.

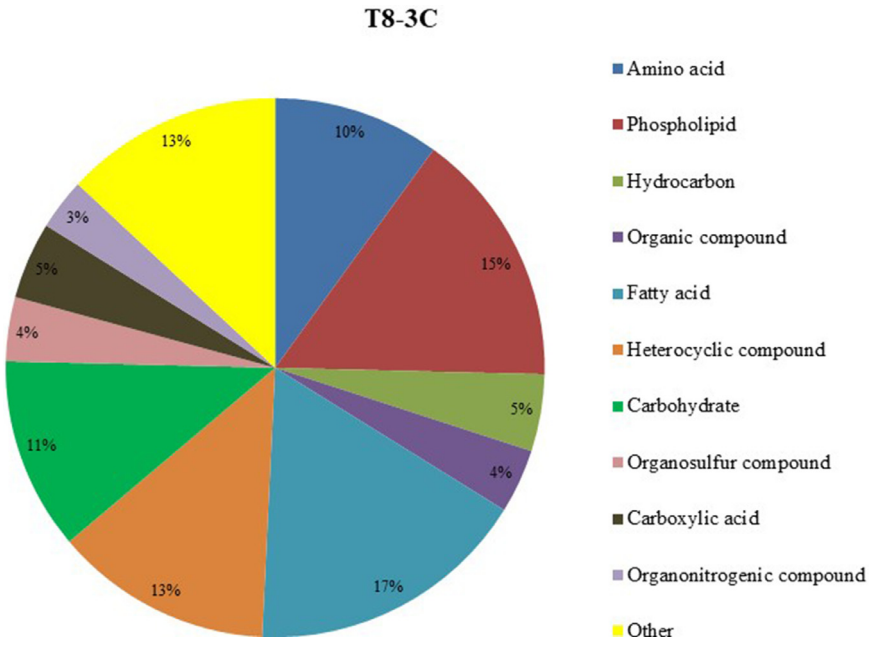

Fig. 17. Distribution of components of *S. boulardii* T8-3C as a result of QTOF-LC/MS.

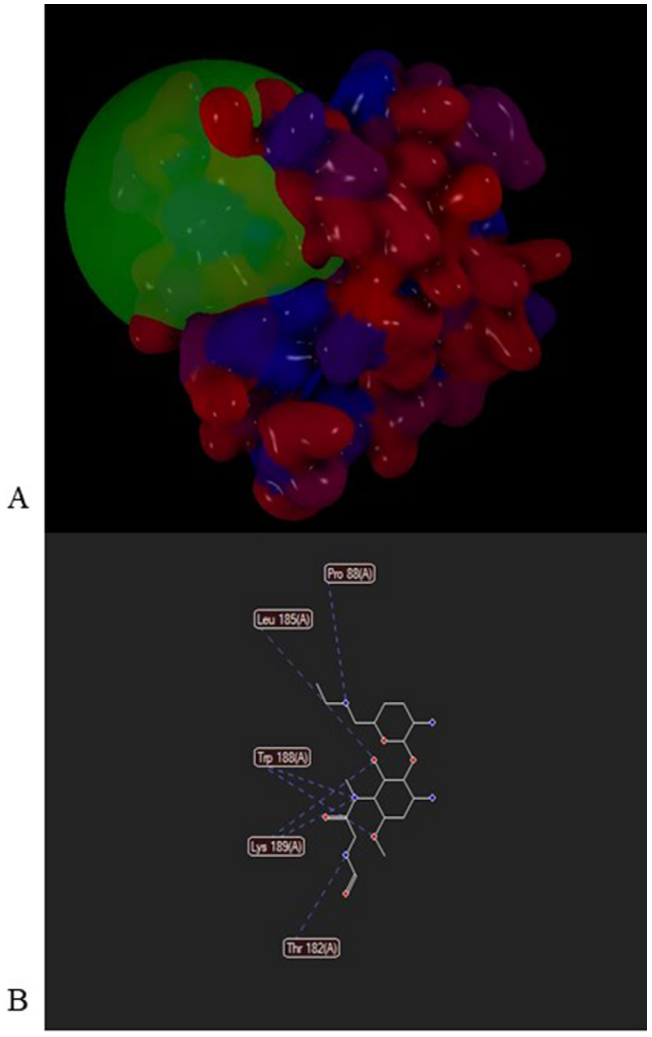

Fig. 18. (A) Interaction between *BAX* protein and istamycin C1 ligand and (B) H bond location.

3.8. Molecular dynamics simulation study

RSMD is an important parameter used for maintaining the stability of backbone atoms of proteins and ligand-protein complexes. The RMSD graph of the metabolite istamycin C1, which best preserves its stability when bound with protein, is given in Fig. 19.

Table 4
Results of molecular docking of irinotecan with target proteins.

Protein	Binding Energy (kcal/mol)	Number of H Bonds	H Bonds Position
BAX	-8.03	6	Ala183 Trp18 Phe92 Arg89 Thr186 Val91
BCL-2	-7.39	7	Ala146 Gly142 Phe147 Phe148 Phe150 Tyr308 Val145
BRAF	-8.53	0	-
CASP3	-8.34	2	Ser267 Val266
CASP8	-8.70	0	-
NF-κB	-7.16	5	Asp26 Phe27 Ser28 Val23 Val24
p53	-8.16	2	Asn345 Phe341

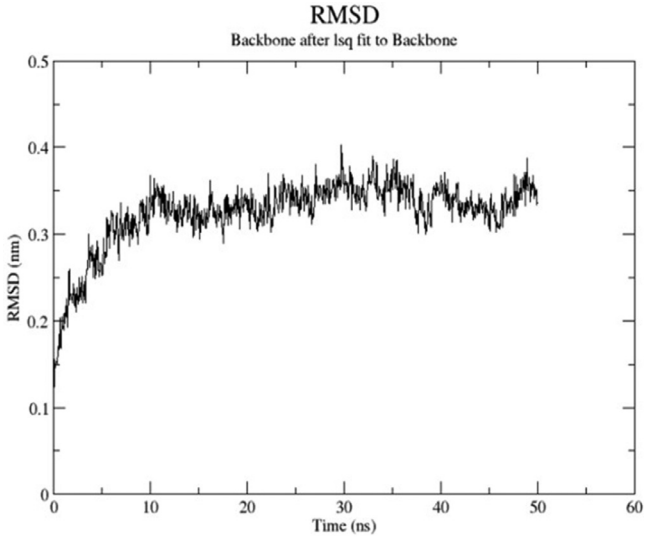

Fig. 19. Istamycin C1 and *BAX* molecular dynamic results.

4. Conclusion

Probiotics are used as preventative or therapeutic agents for cancer tharapy. Many studies show the effectiveness of *L. plantarum* metabolites on cancer cells [50–54]. The findings obtained from the study showed that microorganisms with probiotic properties can play a role as an anticancer agent for the treatment of three important types of cancer. In the study, in addition to *in vitro* experiments, gene expression analyses were also carried out to support the results. At the same time, molecular docking and molecular dynamics simulation studies, which have an important place in drug development studies, have been carried out, and the potential of metabolites produced by probiotic microorganisms to be drugs in cancer treatment has been examined in detail.

This study shows that the use of probiotics alone, as well as in combination with chemotherapy drugs, in cancer treatment can contribute to the success of the treatment process with the fewest side effects. However, more studies are needed to elucidate the mechanisms by which probiotics are effective in the cancer process in humans.

Declaration of Competing Interest

The authors declare the following financial interests/personal relationships which may be considered as potential competing interests.

CRediT authorship contribution statement

Seda Yalçınkaya: Formal analysis. **Serap Yalçın Azarkan:** Conceptualization, Methodology, Writing – original draft. **Aynur Gül Karahan Çakmakçı:** Conceptualization, Methodology, Writing – original draft.

Acknowledgment

This work was supported by Scientific Research Fund of the Suleyman Demirel University. Project Number: FDK-2019-6925.

References

[1] T.A. Baudino, Targeted cancer therapy: the next generation of cancer treatment, Curr. Drug Discov. Technol. 12 (2015) 3–20.
[2] J. Gagnière, J. Raisch, J. Veziant, N. Barnich, R. Bonnet, E. Buc, M.A. Bringer, D. Pezet, M. Bonnet, Gut microbiota imbalance and colorectal cancer, World J. Gastroenterol. 22 (2016) 501–518.
[3] P. Louis, G.L. Hold, H.J. Flint, The gut microbiota, bacterial metabolites and colorectal cancer, Nat. Rev. Microbiol. 12 (2014) 661–672.
[4] I. Kahouli, C. Tomaro-Duchesneau, S. Prakash, Probiotics in colorectal cancer (CRC) with emphasis on mechanisms of action and current perspectives, J. Med. Microbiol. 62 (2013) 1107–1123.
[5] M. Kahraman, A.G. Karahan, Tumor suppressor effects of probiotics, Turk Hij. Den. Biyol. Derg. 75 (2018) 421–442.
[6] E.L. Low, A.E. Simon, J. Lyons, D. Romney-Alexander, J. Waller, What do British women know about cervical cancer symptoms and risk factors? Eur. J. Cancer 48 (2012) 3001–3008.
[7] H.L. Bowyer, R.H. Dodd, L.A.V. Marlow, J. Waller, Association between human papillomavirus vaccine status and other cervical cancer risk factors, Vaccine 32 (2014) 4310–4316.
[8] M.S. Riaz Rajoka, H. Zhao, Y. Lu, Z. Lian, N. Li, N. Hussain, D. Shao, M. Jin, Q. Li, J. Shi, Anticancer potential against cervix cancer (HeLa) cell line of probiotic: *Lactobacillus casei* and *Lactobacillus paracasei* strains isolated from human breast milk, Food Funct. 9 (2018) 2705–2715.
[9] M. Narisawa-Saito, T. Kiyono, Basic mechanisms of high-risk human papillomavirus-induced carcinogenesis: roles of E6 and E7 proteins, Cancer Sci. 98 (2007) 1505–1511.
[10] G. Başyiğit, A.G. Karahan, M.L. Çakmakçı, Probiyotik olma özelliği taşıyan laktik asit bakterilerinin dondurma üretiminde kullanılması, Gıda 30 (2005) 419–424.
[11] M. Kahraman, Probiyotik Özellik Gösteren Bazı Laktik asit Bakterileri ve Mayaların Tümör Baskılayıcı Etkilerinin Araştırılması, Süleyman Demirel Üniversitesi, 2020.
[12] H. Yıldıran, Probiyotik Özellik Gösteren bazı Maya Suşları ve Laktik asit Bakterilerinin Etkileşimlerinin Araştırılması, Süleyman Demirel University, 2017.
[13] M.E.S.J.C. De Man, M. Rogosa, A readily prepared medium for the cultivation of the lactobacilli, J. Bacteriol. 51 (1960) 560.
[14] L.K. Nakamura, Lactobacillus: yeast interrelationships, J. Bacteriol. 81 (1960) 519–523.
[15] A. Gil de la Fuente, J. Godzien, M. Fernández López, F.J. Rupérez, C. Barbas, A. Otero, Knowledge-based metabolite annotation tool: CEU mass mediator, J. Pharm. Biomed. Anal. 154 (2018) 138–149.
[16] R. Foty, A simple hanging drop cell culture protocol for generation of 3D spheroids, J. Vis. Exp. 20 (2011) 4–7.
[17] Y. Qu, B. Han, Y. Yu, W. Yao, S. Bose, B.Y. Karlan, A.E. Giuliano, X. Cui, Evaluation of MCF10A as a reliable model for normal human mammary epithelial cells, PLoS One 10 (2015) 1–16.
[18] J.Y. Kim, T.T.P. Dao, K. Song, S.B. Park, H. Jang, M.K. Park, S.U. Gan, Y.S. Kim, *Annona muricata* leaf extract triggered intrinsic apoptotic pathway to attenuate cancerous features of triple negative breast cancer MDA-MB-231 evidence-based complement, Cells. Evid. Based Complement Alternat. Med. 2018 (2018) 7972916.
[19] L.M. Shaw, Tumor cell invasion assays, Methods Mol. Biol. 294 (2005) 97–105.
[20] https://www.rcsb.org/, RCSB PDB: homepage, (n.d.). https://www.rcsb.org/ (accessed May 21, 2021).
[21] Https://pubchem.ncbi.nlm.nih.gov/, PubChem, (n.d.). https://pubchem.ncbi.nlm.nih.gov/ (accessed May 21, 2021).
[22] O. Trott, A.J. Olson, AutoDock Vina: improving the speed and accuracy of docking with a new scoring function, efficient optimization, and multithreading, J. Comput. Chem. 31 (2009) NA-NA.
[23] WebGro, (2021). https://simlab.uams.edu/index.php (accessed September 25, 2021).
[24] H. Bekker, H. Berendsen, E. Dijkstra, S. Achterop, R. Van Drunen, D. Van der Spoel, A. Sijbers, H. Keegstra, B. Reitsma, M. Renardus, Gromacs: a parallel computer for molecular dynamics simulations, Phys. Comput. 92 (1993) 252–256.
[25] C. Oostenbrink, A. Villa, A.E. Mark, W.F. Van Gunsteren, A biomolecular force field based on the free enthalpy of hydration and solvation: the GROMOS force-field parameter sets 53A5 and 53A6, J. Comput. Chem. 25 (2004) 1656–1676.
[26] E. Lindahl, P. Bjelkmar, P. Larsson, M.A. Cuendet, B. Hess, Implementation of the charmm force field in GROMACS: analysis of protein stability effects from correction maps, virtual interaction sites, and water models, J. Chem. Theory Comput. 6 (2010) 459–466.
[27] K. Lindorff-Larsen, S. Piana, K. Palmo, P. Maragakis, J.L. Klepeis, R.O. Dror, D.E. Shaw, Improved side-chain torsion potentials for the Amber ff99SB protein force field, Proteins Struct. Funct. Bioinform. 78 (2010) 1950–1958.
[28] M.J. Abraham, T. Murtola, R. Schulz, S. Páll, J.C. Smith, B. Hess, E. Lindahl, G. ScienceDirect, High performance molecular simulations through multi-level parallelism from laptops to supercomputers, SoftwareX 1 (2015) 19–25.
[29] V. Bharti, A. Mehta, S. Singh, N. Jain, L. Ahirwal, Cytotoxicity of live whole cell, heat killed cell and cell free extract of lactobacillus strain in U-87 human glioblastoma cell line and MCF-7 breast cancer cell line, Int. J. Probiotics Prebiotics 10 (2015) 153–158.
[30] M.H. Bibalan, M. Eshaghi, M. Rohani, M. Esghaei, D. Darban-Sarokhalil, M.R. Pourshafie, M. Talebi, Isolates of *Lactobacillus plantarum* and *L. Reuteri* display greater antiproliferative and antipathogenic activity than other *Lactobacillus* isolates, J. Med. Microbiol. 66 (2017) 1416–1420.
[31] R. Sambrani, J. Abdolalizadeh, L. Kohan, B. Jafari, Saccharomyces cerevisiae inhibits growth and metastasis and stimulates apoptosis in HT-29 colorectal cancer cell line, Comp. Clin. Pathol. 28 (2018) 985–995.

[32] J. Lee, J.E. Lee, S. Kim, D. Kang, H.M. Yoo, Evaluating cell death using cell-free supernatant of probiotics in three-dimensional spheroid cultures of colorectal cancer cells, J. Vis. Exp. (2020) 1–17.
[33] W. Lim, S. Park, molecules a microfluidic spheroid culture device with a concentration gradient generator for high-throughput screening of drug efficacy, Molecules 23 (2018).
[34] F. Shang, X. Jiang, H. Wang, S. Chen, X. Wang, Y. Liu, S. Guo, D. Li, W. Yu, Z. Zhao, G. Wang, The inhibitory effects of probiotics on colon cancer cells: *in vitro* and *in vivo* studies, J. Gastrointest. Oncol. 11 (2020) 1224–1232.
[35] N. Khoury, S. El-Hayek, O. Tarras, M. El-Sabban, M. El-Sibai, S. Rizk, Kefir exhibits anti-proliferative and pro-apoptotic effects on colon adenocarcinoma cells with no significant effects on cell migration and invasion, Int. J. Oncol. 45 (2014) 2117–2127.
[36] A. Somaida, I. Tariq, G. Ambreen, A.M. Abdelsalam, A.M. Ayoub, M. Wojcik, J.P. Dzoyem, U. Bakowsky, Potent cytotoxicity of four cameroonian plant extracts on different cancer cell lines, Pharmaceuticals 13 (2020) 1–19.
[37] X.F. Wang, J. Du, T.L. Zhang, Q.M. Zhou, Y.Y. Lu, H. Zhang, S.B. Su, Inhibitory effects of PC-SPESII herbal extract on human breast cancer metastasis, evidence-based complement, Altern. Med. 2013 (2013) 11.
[38] Y. Sun, X. Wang, Q. Zhou, Y. Lu, H. Zhang, Q. Chen, M. Zhao, S. Su, Inhibitory effect of emodin on migration, invasion and metastasis of human breast cancer MDA-MB-231 cells *in vitro* and *in vivo*, Oncol. Rep. 33 (2015) 338–346.
[39] Z. Nouri, F. Karami, N. Neyazi, M.H. Modarressi, R. Karimi, M.R. Khorramizadeh, B. Taheri, E. Motevaseli, Dual anti-metastatic and anti-proliferative activity assessment of two probiotics on HeLa and HT-29 cell lines, Cell J. 18 (2016) 127–134.
[40] B. Pakbin, S. Pishkhan Dibazar, S. Allahyari, M. Javadi, A. Farasat, S. Darzi, Probiotic *Saccharomyces cerevisiae var. boulardii* supernatant inhibits survivin gene expression and induces apoptosis in human gastric cancer cells, Food Sci. Nutr. 9 (2020) 692–700.
[41] P. Venkatachalam, V.K. Nadumane, Modulation of *BAX* and Bcl-2 genes by secondary metabolites produced by Penicillium rubens JGIPR9 causes the apoptosis of cancer cell lines, Mycology 12 (2021) 69–81.
[42] Y. Wan, Y. Xin, C. Zhang, D. Wu, D. Ding, L. Tang, L. Owusu, J. Bai, W. Li, Fermentation supernatants of lactobacillus delbrueckii inhibit growth of human colon cancer cells and induce apoptosis through a caspase 3-dependent pathway, Oncol. Lett. 7 (2014) 1738–1742.
[43] Y. Gamallat, A. Meyiah, E.D. Kuugbee, A.M. Hago, G. Chiwala, A. Awadasseid, D. Bamba, X. Zhang, X. Shang, F. Luo, Y. Xin, Lactobacillus rhamnosus induced epithelial cell apoptosis, ameliorates inflammation and prevents colon cancer development in an animal model, Biomed. Pharmacother. 83 (2016) 536–541.
[44] H.S. Roth, P.J. Hergenrother, Derivatives of procaspase-activating compound 1 (PAC-1) and anticancer activities, Curr. Med. Chem. 23 (2016) 201–241.
[45] P.W. Lucas, J.M. Schmit, Q.P. Peterson, D.C. West, D.C. Hsu, C.J. Novotny, L. Dirikolu, M.I. Churchwell, D.R. Doerge, L.D. Garrett, P.J. Hergenrother, T.M. Fan, Pharmacokinetics and derivation of an anticancer dosing regimen for PAC-1, a preferential small molecule activator of procaspase-3, in healthy dogs, Investig. New Drugs 29 (2011) 901–911.
[46] C.P. Wu, S. Lusvarghi, P.J. Tseng, S.H. Hsiao, Y.H. Huang, T.H. Hung, S.V Ambudkar, MY-5445, a phosphodiesterase type 5 inhibitor, resensitizes ABCG2-overexpressing multidrug-resistant cancer cells to cytotoxic anticancer drugs, 1 (2020) 1–18.
[47] J.M. Solomon, R. Pasupuleti, L. Xu, T. Mcdonagh, R. Curtis, P.S. Distefano, L.J. Huber, Inhibition of SIRT1 catalytic activity increases p53 acetylation but does not alter cell survival following DNA damage, Mol. Cell. Biol. 26 (2006) 28–38.
[48] S. Sampath, S. Subramani, S. Janardhanam, P. Subramani, A. Yuvaraj, R. Chellan, Bioactive compound 1,8-cineole selectively induces G2/M arrest in A431 cells through the upregulation of the p53 signaling pathway and molecular docking studies, Phytomedicine 46 (2018) 57–68.
[49] F.K. Ata, S. Yalçın, F. Ercan, in: Docking Studies of Metabolites of Annona Muricata and Abemaciclib on Human BCL-2, Bad and AKT1 Proteıns, Kırşehir Ahi Evran University Thesis, 2019, pp. 251–253.
[50] C.H.K. Momo, A.D.K. Mboussaah, N. François Zambou, M.A. Shaiq, New pyran derivative with antioxidant and anticancer properties isolated from the probiotic *Lactobacillus plantarum* H24 strain, Nat. Prod. Res. 36 (2022) 909–917.
[51] M. Sun, W. Liu, Y. Song, Y. Tuo, G. Mu, F. Ma, The effects of *Lactobacillus plantarum*-12 crude exopolysaccharides on the cell proliferation and apoptosis of human colon cancer (HT-29) cells, Probiotics Antimicrob. Proteins 13 (2021) 413–421.
[52] W. Dwi Ningtiyas, I. Isnafia Arief, C. Budiman, A.R. Handoyo Utomo, Inhibition of human cervical cancer HeLa cell line by meat-derived lactic acid bacteria of *Lactobacillus plantarum* IIA-1A5 and *Lactobacillus acidophilus* IIA-2B4, Pak. J. Biol. Sci. 24 (2021) 1340–1349.
[53] H.J. Kim, J. An, E.M. Ha, *Lactobacillus plantarum*-derived metabolites sensitize the tumor-suppressive effects of butyrate by regulating the functional expression of SMCT1 in 5-FU-resistant colorectal cancer cells, J. Microbiol. 60 (2022) 100–117.
[54] M. Sentürk, F. Ercan, S. Yalcin, The secondary metabolites produced by *Lactobacillus plantarum* downregulate BCL-2 and BUFFY genes on breast cancer cell line and model organism drosophila melanogaster: molecular docking approach, Cancer Chemother. Pharmacol. 85 (2020) 33–45.